INEEL/CON-98-00338
PREPRINT

Imaging Of Lamb Waves In Plates For Quantitative Determination Of Anisotropy Using Photorefractive Dynamic Holography

K. L. Telschow
V. A. Deason
R. S. Schley
S. M. Watson

June 19, 1998

25th Annual Review Of Progress In Quantitative Nondestructive Examination

IMAGING OF LAMB WAVES IN PLATES FOR QUANTITATIVE DETERMINATION OF ANISOTROPY USING PHOTOREFRACTIVE DYNAMIC HOLOGRAPHY

K.L. Telschow, V. A. Deason, R. S. Schley and S. M. Watson
Idaho National Engineering and Environmental Laboratory
Lockheed Martin Idaho Technologies Co.
Idaho Falls, ID 83415-2209

INTRODUCTION

Anisotropic properties of sheet materials can be determined by measuring the propagation of Lamb waves in different directions. Electromagnetic acoustic transduction and laser ultrasonic methods provide noncontacting approaches that are often desired for application to industrial and processing environments. This paper describes a laser imaging approach utilizing the adaptive property of photorefractive materials to produce a real-time measurement of the antisymmetric Lamb wave mode in all directions simultaneously. Continuous excitation is employed enabling the data to be recorded and displayed by a CCD camera. Analysis of the image produces a direct quantitative determination of the phase velocity in all directions showing plate anisotropy in the plane.

Many optical techniques for measuring ultrasonic motion at surfaces have been developed for use in applications such as vibration measurement and laser ultrasonics. Most of these methods have similar sensitivities and are based on time domain processing using homodyne, Fabry-Perot [1], and, more recently, photorefractive interferometry [2]. Generally, the methods described above do not allow measurement at more than one surface point simultaneously, requiring multiple beam movements and scanning in order to produce images of surface ultrasonic motion over a large area. Electronic speckle interferometry, including shearography, does provide images directly of vibrations over large surface areas. This method has proven very durable in the field for large displacement amplitudes of several wavelengths. In addition, a sensitivity of $\lambda/3000$ has been demonstrated under laboratory conditions [3]. Full-field imaging of traveling ultrasonic waves using digital shearography has been recently reported with sensitivity in the nanometer range [4]. With this method, optical interference occurs at the photodetector

surface of the camera that records the speckle image from the surface. Multiple image frames are typically recorded and processed in a computer to produce an output proportional to surface displacement. This paper discusses a powerful alternative method that utilizes the photorefractive effect in optically nonlinear materials to perform adaptive interferometry [5,6]. Optical interference occurs within the photorefractive material with this technique and the output is configured to be an optical beam whose intensity is directly proportional to the surface vibration amplitude for small ultrasonic displacements. Utilizing this approach, no post-processing is required to produce images of the surface vibration amplitude over large areas. The fundamental approach and application to standing wave imaging of resonant motion in plates have been previously described [7-9]. This paper describes the extension of this technique to non-stationary waveforms through imaging of traveling Lamb waves in plates.

BACKGROUND

Photorefractivity employs optical excitation and transport of charge carriers that are produced from the interference pattern developed inside specific materials. A spatial and temporal charge distribution results that reflects the phase information impressed onto the optical signal beam by the vibrating surface. Several optical frequency domain measurement methods of vibration have been proposed using photorefractive two and four-wave mixing in select materials [7-12]. Some of these provide a time averaged response that is a nonlinear function of the specimen vibration displacement amplitude. The method reported here measures the photorefractive grating produced at a fixed beat frequency between the phase modulated signal and reference beams. It can be used in a manner that directly measures vibration amplitude and phase with a response proportional to the Bessel function of order one, providing a direct output linear for small amplitudes. The method accommodates rough surfaces, exhibits a flat frequency response above the photorefractive response cutoff frequency and can be used for detecting both standing and traveling waves.

MEASUREMENTS OF TRAVELING WAVES

The experimental setup for traveling wave point detection is shown in figure 1. A diode pumped solid state laser source at 532 nm, 5 W, was split into two legs for signal and reference beams. The signal beam was reflected off a specimen plate driven continuously at its center by a piezoelectric transducer. Flexural waves (lowest order antisymmetric Lamb modes) traveled radially outward from the center and were attenuated at the plate edges through contact with an absorbing material preventing standing wave behavior. The traveling wave displacement at the plate surface modulated the phase (δ_{sig}) of the signal beam as shown in figure 1. The reference beam was phase modulated by an electro-optic modulator at a fixed modulation depth (δ_{ref}). The modulated beams were then combined and interfered inside a bismuth silicon oxide (BSO) photorefractive crystal as shown. The photorefractive crystal was 10 mm by 10 mm by 2.25 mm and cut along the <001> and <011> directions. A high extinction ratio polarizer selected one component of the signal beam from the specimen. At the output of the crystal, the diffracted wavefront was selected through another high extinction ratio polarizer. A narrow beam diameter of about 2 mm was used for making point measurements, while the beam was expanded to cover roughly a 50

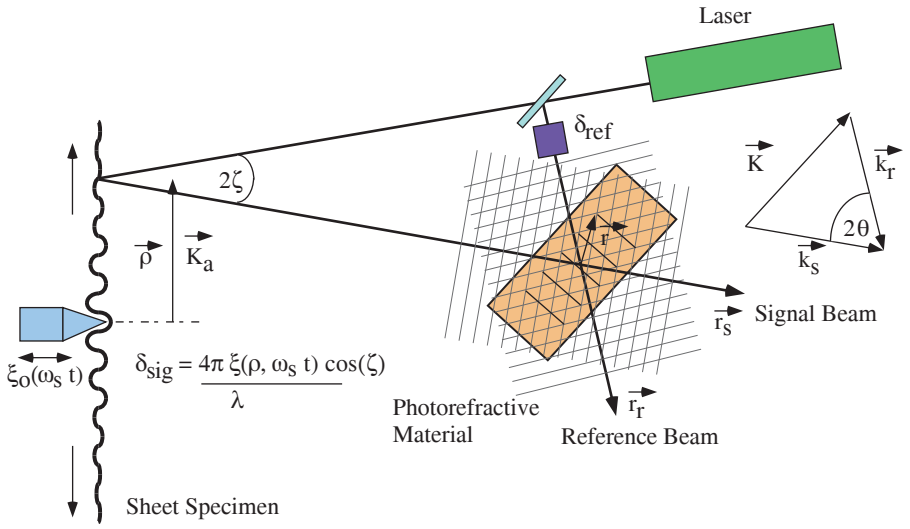

Figure 1. Basic 2-wave mixing geometry for dynamic photorefractive holographic measurement of traveling waves at the surface of a plate.

mm diameter on the plate for imaging. Subsequently, a photodetector, coupled with conventional electrical lock-in methods, recorded the point measurement displacement amplitude and phase or an image was captured with a CCD camera at 30 Hz frame rates.

Point Measurements

Single point measurements were performed by scanning a narrow signal beam across the plate surface along a radius. The lock-in demodulated signal provided both the amplitude and phase at each measurement point. Even though the wave was not stationary, the amplitude and phase results can be recorded to show the wave motion as a time frozen picture of the spatial waveform in figure 2. The lowest antisymmetric Lamb wave mode, with wavevector K_a, was excited at the origin of an isotropic nickel plate, thickness

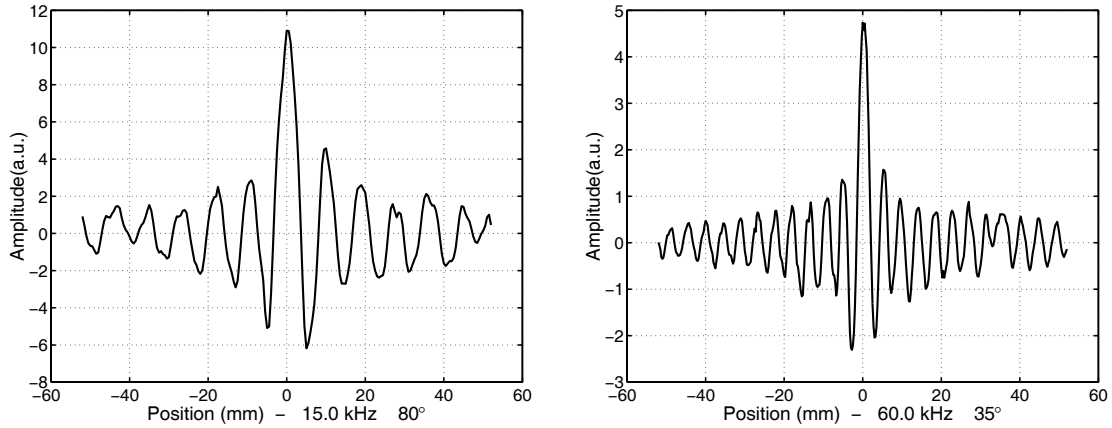

Figure 2. Captured waveforms of traveling waves driven at the center of a nickel plate at two different frequencies showing the corresponding change in wavelength. The phase shift of the waveform with respect to the piezoelectric source is shown in the caption.

0.13mm, by a piezoelectric transducer undergoing continuous oscillation with amplitude $\xi_p = \xi_0 \sin(\omega_s t + \varphi_s)$. In the far field $K_a \rho > 1$, the normal displacement of the wave traveling radially outward from the excitation point is given by [13]

$$\xi(\rho,t) \approx \xi_m(\rho)\, e^{i(K_a \rho - \omega_s t - \varphi_s + \frac{\pi}{4})}, \qquad \xi_m(\rho) \equiv \xi_0 \sqrt{\frac{2}{\pi K_a \rho}} \tag{1}$$

with the antisymmetric mode wavevector and wavelength given by $K_a = \frac{2\pi}{\Lambda_a}$, $\Lambda_a = \frac{C_a}{\omega_s}$. The antisymmetric mode phase velocity, C_a, is well known from the elastic theory for plate waves and allows the wavelength to be predicted based on given material elastic constants.

The optical phase of the signal beam reflected from the measurement point on the plate surface is modulated by the traveling wave according to $\delta_{sig}(\rho,t) = \frac{4\pi\xi(\rho,t)}{\lambda}\cos(\zeta)$, where ζ is the angle between the surface normal and the signal beam. The optical reference beam is phase modulated by the electro-optic modulator as $\delta_{ref} = \delta_{r0} \sin(\omega_r t + \varphi_r)$. Interference inside the crystal produced a spatially and temporally modulated intensity pattern that was processed by the photorefractive effect to produce an output beam with intensity proportional to

$$\left[\frac{4J_0(\delta_{r0})J_1(\delta_{r0})}{\sqrt{1+\Omega^2\tau^2}}\right] J_0\left(\frac{4\pi\xi_m(\rho)}{\lambda}\right) J_1\left(\frac{4\pi\xi_m(\rho)}{\lambda}\right) \cos(\Omega t + \Phi - K_a\rho - \psi) \tag{2}$$

where the frequency difference $\Omega = \omega_r - \omega_s$, the phase difference $\Phi = \varphi_r - \varphi_s$, J_n is the Bessel function of the first kind and $\tan(\psi) = \Omega\tau$. In the above configuration, the photorefractive crystal acts as a mixing and low pass filtering element demodulating the traveling wavefront into a time varying index modulation and an output beam with intensity that contains both the amplitude and phase information of the wavefront. The space charge field responds only to slowly varying phase modulations occurring within the material response time constant allowing only the terms around the difference frequency, $\Omega << \omega_{s,r}$.

The flexural mode wavelength Λ_a can be determined from the signal phase allowing determination of the plane wave dispersion for this mode. Figure 3 shows the good agreement achieved between the measured and predicted wavelengths over a large frequency range using known elastic constants for the nickel plate.

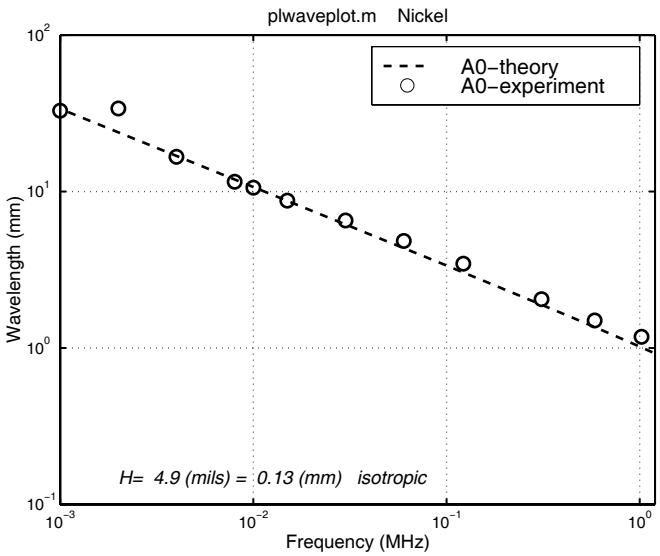

Figure 3. Wavelength of the traveling Lamb mode as a function of frequency compared to that predicted using known elastic constants for the 0.13 mm thick nickel plate.

Imaging Measurements

Since the detection mechanism is holographic, the optical interference and the photorefractive effect allow the point method described above to be extended to image the ultrasonic motion over a large surface area of the plate. The distributed character of the photorefractive holographic process creates a grating distribution that corresponds to the phase modulation at all points on the specimen surface simultaneously. The output beam intensity can then be measured by an array of detectors, or even a highly pixelated device, such as a CCD camera. This capability for imaging is a significant feature of the photorefractive lock-in measurement technique that offers advantages for implementation in a field environment. Figure 4 shows images of the traveling wave modes of the nickel plate obtained with the two-wave mixing method. The flexural mode wavefronts traveling

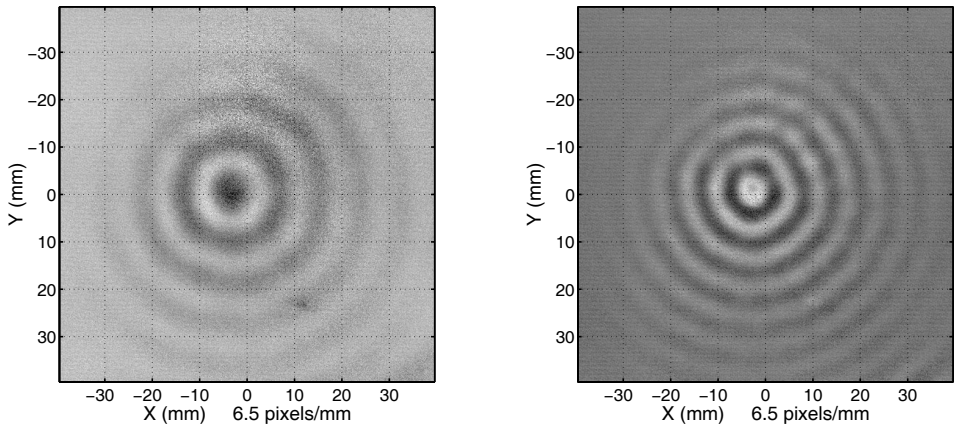

Figure 4. Images of traveling Lamb waves in nickel at 15 kHz (left) and 30 kHz (right).

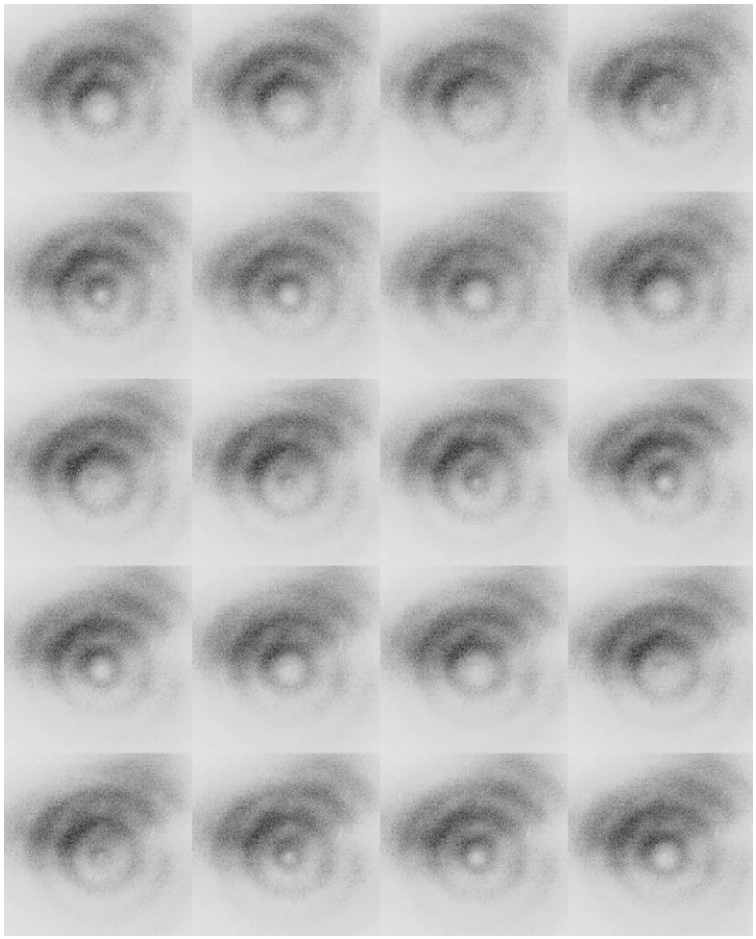

Figure 5. Time-lapse picture of successive frames of the traveling wave images showing the emergence of the wavefront from the center of the plate.

outward from the center are clearly defined, and the relative phase of the displacements is readily distinguishable. The figure shows image data frames at two different frequencies that have the background subtracted. For qualitative inspection of two dimensional waveforms from the CCD output, the eye integrates over multiple video frames. This makes it possible to easily detect subtle patterns that might not be as easily extracted by digital image processing methods. Also the entire pattern can be made to change its phase continuously at the frequency, Ω, perhaps about 2 Hz, so that the appearance is that of waves emanating from the center and traveling outward. This is physically equivalent to the actual traveling wave motion except that viewing of the wave has been slowed to a much smaller observation frequency that is held constant and independent of the actual wave frequency. The photorefractive process yields a true picture of the actual wave vertical displacement motion and does not require any additional processing to generate the images of figure 4.

A sequence of many successive frames is shown in figure 5. The frame rate is 30 Hz and the offset frequency is about 2 Hz resulting in a continuous change in the relative phases between each image. The result is a time-lapse image that shows the viewer a wave

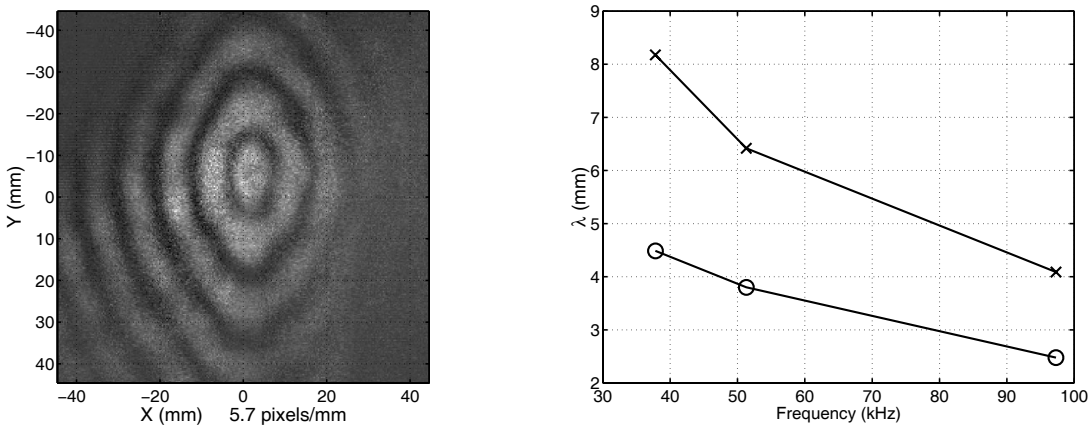

Figure 6. Traveling wave in a an anisotropic composite sheet at 37.8 kHz. Measurements of the wavelength in the vertical and horizontal directions are shown to the right.

emanating from the center and traveling outward and finally attenuated outside the field of view. This quasi-real-time imaging tells the viewer the wavefront shape from which the wavelength and the locations of flaws along the wave path can be determined.

If the specimen is elastically anisotropic, then the wave speed varies with the propagation direction. Figure 6 shows this type of behavior for traveling waves in a sheet of carbon fiber composite. The carbon fiber sheet was approximately 0.178 mm thick with the fibers aligned in parallel along the vertical direction. The matrix is an isotropic resin material. The highly oblong wavefront pattern seen in figure 6 shows the anisotropy clearly and immediately. The right frame of figure 6 shows the wavelengths measured for this composite sheet in the directions along (x's) and perpendicular (o's) to the fibers as a function of frequency. Clearly, a great deal of information about the anisotropic elastic properties of the sheet can be obtained directly from this image measurement technique.

CONCLUSIONS

A photorefractive optical lock-in traveling wave measurement method has been described. Two-wave mixing was employed for reading out the signal producing an output intensity directly proportional to the amplitude of the vibration being measured at a preset mechanical phase. Point measurements scanned along a propagation radius produce a spatial snapshot of the amplitude and phase of the traveling waveform. Direct two-dimensional surface images of the traveling wave were obtained by expanding the collection optics and imaging the output beam from the photorefractive material. These images show the ultrasonic wavelength and wavefront shape and provide a quantitative method for obtaining the thickness, elastic properties and anisotropy of sheet materials, as illustrated for an anisotropic composite carbon sheet. The method is capable of flat frequency response over a wide range above the cutoff of the photorefractive effect and is applicable to rough surfaces.

ACKNOWLEDGMENTS

This work was sponsored by the U.S. Department of Energy, Office of Energy Research, Office of Basic Energy Sciences and the INEEL Laboratory Directed Research & Development program under DOE Idaho Operations Office Contract DE-AC07-94ID13223.

VI REFERENCES

1. J. W. Wagner, "Optical Detection of Ultrasound," *Physical Acoustics*, Vol.XIX, Eds. Thurston, R.N., and Pierce, A.D., (Academic Press, New York, 1990) Ch. 5.
2. R. K. Ing and J.-P. Monchalin, Appl. Phys. Lett. 59, 3233 (1991).
3. S. Ellingsrud and G.O.Rosvold, J. Opt. Soc. Am. A 9 (2), 237-251 (1992).
4. B. A. Bard, G. A. Gordon, and S. Wu, J. Acoust. Soc. Am. 103 (6), 3327-3335, 1998.
5. P. Yeh, *Introduction to Photorefractive Nonlinear Optics*, (John Wiley, New York, 1993).
6. S. I. Stepanov, *International Trends inOptics*, (Academic Press, New York, 1991) Ch. 9
7. T. C. Chatters and K. L. Telschow, *Review of Progress in QNDE*, Vol.15B, Eds. D.O. Thompson and D.E. Chimenti, (Plenum Press, New York, 1996) pp. 2165-2171.
8. T.C. Hale and K. Telschow, Appl. Phys. Lett. 69, 2632-2634 (1996).
9. T.C. Hale, K.L. Telschow and V.A. Deason, Applied Optics, 111, 8248 – 8258 (1997).
10. J. P. Huignard and A. Marrakchi, Opt. Lett., 6, (12), 622-624 (1981).
11. H. R. Hofmeister and A. Yariv, Appl. Phys. Lett., 61 (20), 2395-2397 (1992).
12. H. Rohleder, P. M. Petersen and A. Marrakchi, J. Appl. Phys., 76 (1), 81-84 (1994).
13. P.M. Morse and K. U. Ingard, *Theoretical Acoustics,* (McGraw-Hill, New York, 1968) 219.